

## Deliverable D12.4: Documentation on the ground-based remote sensing particle flux measurements

**Leena Järvi (UHEL), Lucas Alados Arboledas (UGR), Ronny Engelmann (TROPOS), Holger Baars (TROPOS), Arnoud Apituley (KNMI), Otakar Makes (CHMI), Ewan O'Connor (FMI), Antti Manninen (UHEL), Pyry Pentikäinen (UHEL) and Vladimir Zdimal (CHMI)**

<b>Work package no</b>	<b>WP12</b>
<b>Deliverable no.</b>	<b>D12.4</b>
<b>Lead beneficiary</b>	<b>FMI</b>
<b>Deliverable type</b>	<input checked="" type="checkbox"/> R (Document, report) <input type="checkbox"/> DEC (Websites, patent fillings, videos, etc.) <input type="checkbox"/> OTHER: please specify .....
<b>Dissemination level</b>	<input checked="" type="checkbox"/> PU (public) <input type="checkbox"/> CO (confidential, only for members of the Consortium, incl Commission)
<b>Estimated delivery date</b>	<b>April 30</b>
<b>Actual delivery date</b>	<b>30/4/2018</b>
<b>Version</b>	<b>V1</b>
<b>Comments</b>	<i>R+PU</i>

The exchange of aerosol particles between the atmosphere and the surface plays a significant role in determining the mass and number distribution of atmospheric aerosol particles. The surface exchange is commonly measured using tower-based methods but their downside is that they do not provide information what is happening higher in the atmosphere. The vertical aerosol transport within the planetary boundary layer (PBL) must however be monitored to fully understand the local and background dispersion mechanisms. Such measurements allow the quantification of the surface emission of aerosol particles relevant for haze/smog formation and atmospheric composition, and the vertical transport and mixing of aerosol is integral to understanding the relative impact of local sources when attempting to quantify the link between aerosol and cloud droplet formation.

Vertical profiles of particle fluxes in PBL can be determined from co-located Doppler and aerosol lidars by combining the turbulent vertical-wind component derived from the first instrument with aerosol variance and microphysical properties obtained from the second. During ACTRIS-2, such co-located measurements have been performed in terms of field campaigns at Pallas (FMI, Finland) and Košetice (Czech Republic), in addition to Hyytiälä (Finland), Cabauw (the Netherlands), and AGORA (Spain), where the requirement for horizontal homogeneity for flux measurements and the possibility to compare with in-situ measurements are met. This document will describe details of the different measurement campaigns conducted at the five sites.

### **AGORA and Granada**

In Spain, co-located aerosol and Doppler lidar observations were gathered during the AMAPOLA campaign in an olive orchard (close to Jaen [37° 46' N; 3° 46' W], 573 m asl) from 18 to 29 April 2016. The Halo Streamline Doppler Lidar operates at a wavelength of 1.5  $\mu\text{m}$  with 300 gates. The range gate length was 30 m, so that the first gate was located 60 m above the ground. An aerosol lidar, named Veleta, operated at wavelengths of 355 and 387 nm with a nominal spatial resolution of 7.5 m. The Doppler lidar was operated continuously while the aerosol elastic lidar was operated during daytime at 1 Hz frequency. These two systems were separated by an approximate distance of 3 m. In parallel with the remote system instruments, tower-based particle flux measurements were conducted, gathering 9 days of simultaneous lidar and *in-situ* measurements from the site. The tower setup consisted of an ultrasonic anemometer (RMYoung 81000) and a condensation particle counter (TSI3776). Both instruments measured with a sampling frequency of 10 Hz.

A similar remote sensing setup was also utilized during the Sierra Nevada AerOsol Profiling Experiment (SLOPE-I) campaign performed during May to August 2016 at the Andalusian Institute of Earth System Research (IISTA-CEAMA) in Granada (37.16° N; 3.61° W, 680 m asl). The main difference was the replacement of Veleta lidar with Mulhacen lidar, an aerosol lidar that operates at 355, 387, 408, 532, 607 and 1064 nm with spatial resolution of 7.5 m. Similar to the AMAPOLA campaign deployment, the Doppler lidar was operated continuously while the Mulhacen was operated during daytime at 1 Hz frequency. They were separated by a distance of approximately 3 m. Co-located in addition was a Microwave Radiometer (*MWR*) from which the Planetary Boundary Layer height ( $PBLH_{MWR}$ ) was retrieved (Moreira et al. 2018). Tower-based particle flux measurements were performed at the observation tower of the "Parque de las Ciencias", located 250 m away from the rooftop of the Atmospheric Physics Lab at the Andalusian Institute for Earth System Research IISTA-CEAMA, where remote system instruments are operated (Fig. 1). The sonic anemometer and the inlet to the CPC are located on top of the tower, 50 m above the surface. The CPC is located 10 m below, in a shelter equipped with a Peltier cooling system. The main aerosol inlet line works at 15 L min<sup>-1</sup>, using an external pump, and the CPC flow rate is 1.5 L min<sup>-1</sup>.



Figure 1. Experimental set up for the eddy covariance and remotes sensing setups at the urban area of Granada.

Figure 2 describes the methodology utilized to obtain the vertical profile of aerosol mass flux ( $F(z)$ ) from the co-located lidars. The Doppler lidar and aerosol lidar are synchronized in order to acquire vertical wind velocity ( $w$ ) and the range-corrected signal ( $RCS$ ), respectively, at the same instant and with the same time resolution (2 s). The data are averaged in 1-hour packages, from which the mean values ( $\bar{q}(z)$ ) are extracted. The mean values are subtracted from each  $q_n(z)$  profile, providing the fluctuation of vertical profile of measured variable  $q'_n(z)$ :

$$q'_n(z) = q_n(z) - \bar{q}(z). \tag{1}$$

From the fluctuation of  $w'$  it is possible to acquire the vertical profile of integral time scale and skewness, which provide information about the length of vortices and the direction of convection, respectively. The utilization of the Klett method (Klett 1981) on elastic lidar data provides the vertical profile of backscatter coefficient  $\beta(z)$ , which, combined with Sunphotometer data, provides the lidar ratio profile  $S_{532}^p$ . From the combination of  $w'$ ,  $RCS'$ ,  $S_{532}^p$  and Mass extinction coefficient  $MEE_{532}$  (Kinne et al. 2006) it is possible to estimate  $F(z)$  (Engelmann et al., 2007). Figure 3 shows an example of the application of the methodology described in Fig. 1 for 13 July 2016 during SLOPE-I campaign. Figure 2 shows the  $RCS(z)$  profile and the  $PBLH_{MWR}$  (black stars).  $PBLH_{MWR}$  grows at the same rate as the aerosol layers ascend, as expected.

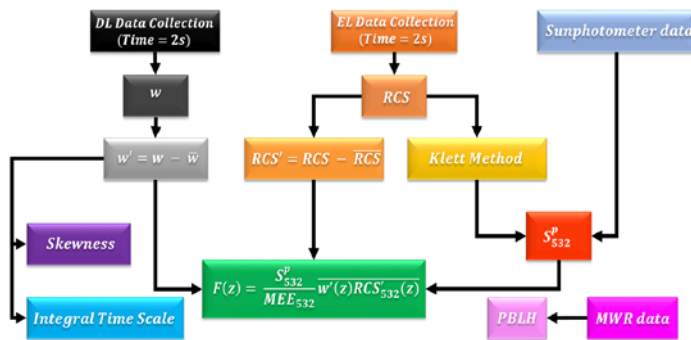


Figure 2. Methodology utilised to obtain vertical profile of aerosol mass flux  $F(z)$ .

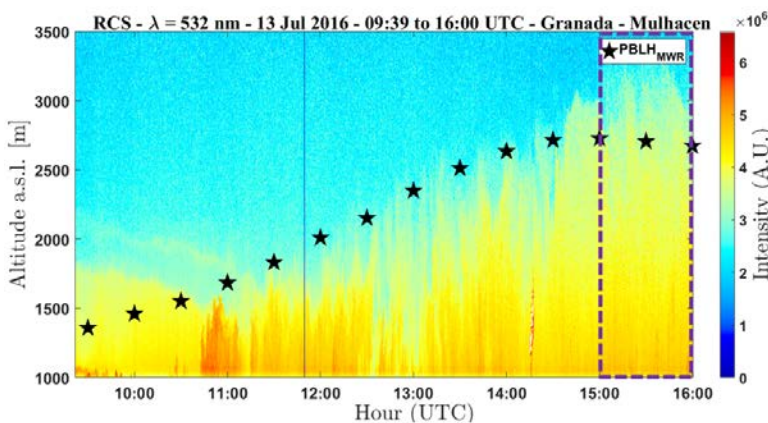


Figure 3. Elastic lidar range-corrected signal ( $RCS(z)$ ) and Planetary Boundary Layer height ( $PBLH_{MWR}$ , black stars) on 13 July 2016. The dashed box indicates the region where the vertical profile of  $F(z)$  is calculated.

Figure 4 shows the values of the integral time scale obtained from  $w'(z)$ . The grey areas indicate regions where the integral time scale has values lower than Doppler lidar acquisition (2 s) and due to instrumental limitations we cannot observe the turbulent movements. However, these regions are concentrated mainly above  $PBLH_{MWR}$ , which is not the main interest of this work. Skewness of  $w'(z)$  is shown in Fig. 5. The Skewness values are in agreement with  $PBLH_{MWR}$  dynamics (ascent when positive values of Skewness are observed and decreasing when Skewness has negative values) and  $RCS(z)$  evolution.

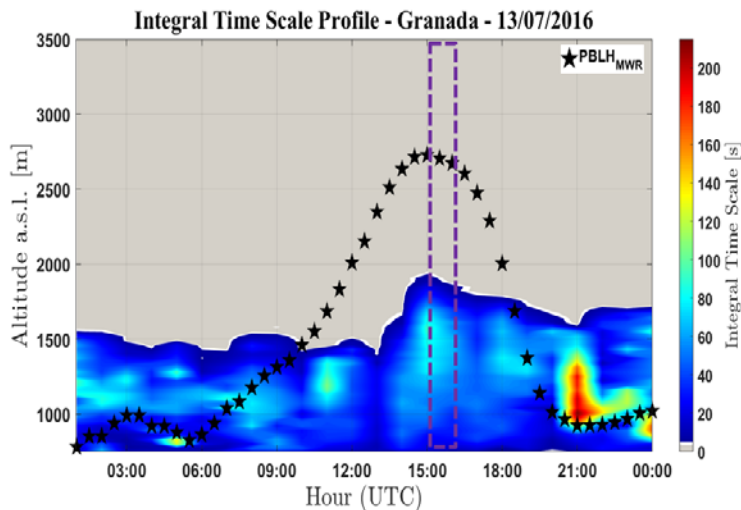


Figure 4. Integral time scale obtained from  $w'(z)$  on 13 July 2016. The dotted purple box indicated the region where  $F(z)$  analysis is performed.

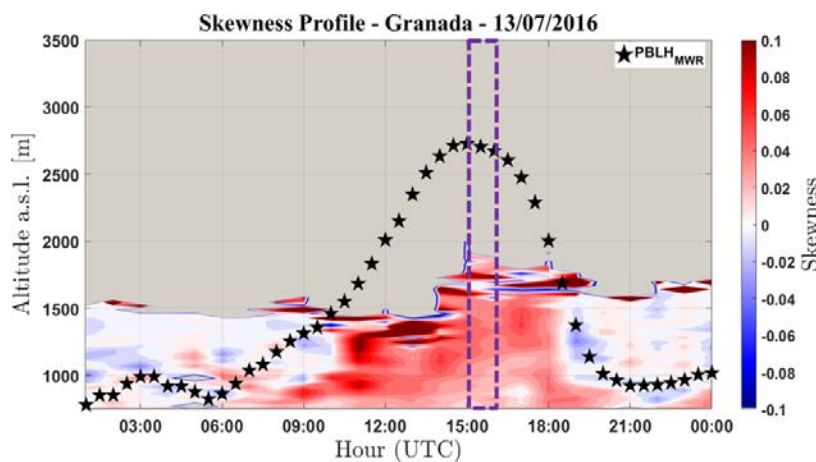


Figure 5. Skewness obtained from  $w'(z)$  on 13 July 2016. The dotted purple box indicated the region where  $F(z)$  analysis is performed.

The aerosol mass flux  $F(z)$  obtained from 15 to 16 UTC is presented in Figure 6. The predominance of positive values are in agreement with the information presented in Figs. 3 and 5. The higher values of  $F(z)$  occur at the same height where higher values of Skewness are observed (Fig. 5).

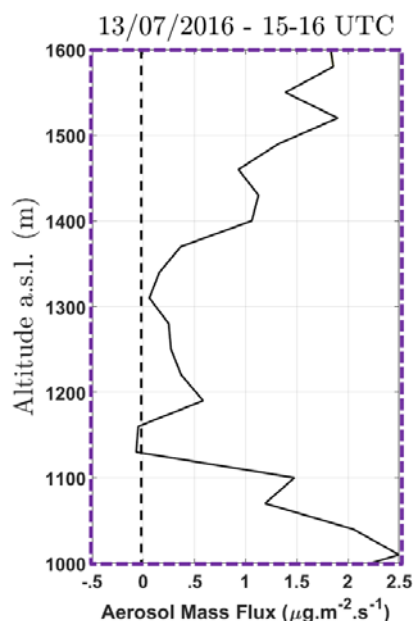


Figure 6. Vertical profile of aerosol mass flux  $F(z)$  on 13 July 2016 for the area shown in Figs. 3-5.

### Cabauw (The Netherlands, KNMI)

The CESAR (*Cabauw Experimental Site for Atmospheric Research*, [www.cesar-observatory.nl](http://www.cesar-observatory.nl)) Observatory is located in the western part of the Netherlands (51.971° N, 4.927° E) in a polder 0.7 m below average sea level. The nearby area is dominated by flat agricultural grassland with relatively little industry and households. In contrast, the wider surrounding area at distances 15 – 50 km away, more than 10 million people live and work in one of the most densely populated areas in Europe. The CESAR Observatory includes a 212 m tall tower specifically built for meteorological and air pollution studies.

Co-located vertical flux measurements were conducted during CINDI-2 campaign in fall 2016. After several attempts to obtain a Doppler wind lidar, the campaign was executed using a Zephir 300 wind lidar. The Zephir 300 is a continuous wave lidar. Although the Zephir has provided wind information, unfortunately this continuous wave lidar was not able to provide wind measurements at sufficient frequency for flux measurements. We also learned that the Zephir could not provide aerosol (backscatter) information with the obtained wind. The high-performance multiwavelength Raman lidar Caeli was operated during the CINDI-2 campaign to provide aerosol backscatter and extinction profiles. Those were available during 10 days of the campaign. Simultaneously with the lidar measurements, a CPC (TSI3775) and a Gill sonic anemometer were measured at the height of 67m height providing in-situ aerosol particle fluxes. The analysis of the data is ongoing.

### Košetice (Czech Republic, CHMI)

The National Atmospheric Observatory Košetice is situated in the agricultural countryside in the Czech Highlands (534 m above sea level). In addition to meteorological parameters, many different air quality ground based parameters are measured at the station ( $PM_{10}$ ,  $PM_{2.5}$ ,  $NO_x$ ,  $NH_x$ ,  $O_3$ ,  $SO_x$ , CO, POPs, VOCs) as well as aerosol characterization (PNSD, light absorption, light scattering, EC/OC). Further measurements (vertical gradients of GHGs,  $O_3$  and Hg) are run at the 250 m high atmospheric tall tower.

During 15 August – 15 September 2017, a lidar measurement campaign took place at the site. A Halo Streamline Doppler lidar was transported to the Observatory from Finland by the Finnish Meteorological Institute, and TROPOS provided a PollyXT aerosol lidar from Germany (Fig. 7). Several additional measurements were set up on the tower to support the lidar campaign. Eddy covariance measurements at a height of 80 m were conducted. The setup comprised a Gill ultrasonic anemometer and CPC (TSI3775) measuring at a frequency of 1 Hz. In addition, an SMPS and APS were deployed at the tower platform at 230 m. An SMPS (TSI CPC 3025 and Electrostatic Classifier 3080 with the long DMA 3081) and APS (TSI 3321) were placed into a ventilated box. Aerosol is sampled into the APS through a mini  $PM_{10}$  (BGI) inlet and 1.5 m long stainless steel tube with  $\frac{1}{2}$  inch diameter. Aerosol for the SMPS was isokinetically subsampled and dried with silica gel diffusion drier. The flow rate for the SMPS was set to  $0.3 \text{ L min}^{-1}$ .



Figure 7. Transport and setup of the Polly-XT OCEANET container from TROPOS to Košetice.

The Polly-XT lidar operated from 14 August to 29 October together with a Spectral Extinction Monitoring System (SAEMS), which measures the aerosol extinction near the surface. The Halo Doppler lidar operated continuously from 16 August to 20 September, providing vertical profiles at 6 s resolution. In addition, the Doppler lidar scan sequence included Velocity-Azimuth-Display (VAD) scans at 15 and 75 degree elevation from horizontal to obtain the horizontal wind profile with 15-minute resolution, and low-level sector scans coincident with SAEMS. The 2<sup>nd</sup> half of August was selected as a good period to compare *in-situ* and lidar derived aerosol fluxes, 23 August is the “Golden Day”. As a first step, we determined the optical profiles of aerosols with Polly XT (Fig. 8). The lidar ratios of 40-50 sr and a depolarization ratio of 3% indicate typical low-absorbing continental aerosol conditions.

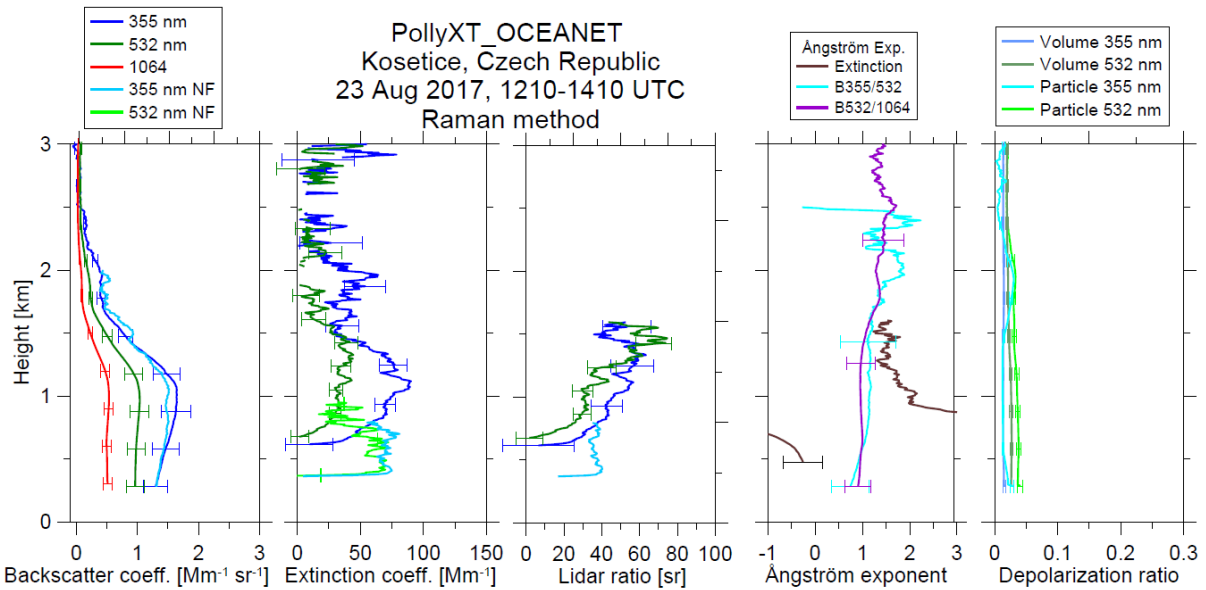


Figure 8. Profiles of optical aerosol properties on 23 August derived from PollyXT.

The PollyXT lidar was also equipped with an analogue channel in order to obtain profiles of the backscatter coefficient at 532 nm with a high temporal resolution (5-10 s). Therefore, we replaced the detector of the near-range 532-nm channel with a Hamamatsu H10721 photomodule, a Femto amplifier HCA-20M-100K-C. The analogue/digital conversion was performed by a 20-MHz USB PICO Scope 5243B. The results of the synchronous highly resolved wind and aerosol measurements for a convective period in the afternoon of 23 August are shown in Fig. 9. Gaps in the vertical velocity field are a result of VAD scans. Updrafts and downdrafts are noted by arrows and indicate already a positive (upward) flux at the top of the boundary layer and a negative (downward) flux at the surface. This means that the “residual layer” functions as a source, where the surface and the free-troposphere are sinks.

Figure 10 shows the first (preliminary) profiles of the vertical aerosol mass flux from lidar measurements in Košetice on 23 August 2018 for three different periods. Currently, the covariance from the backscatter and wind fluctuations was converted into a mass flux by a factor of  $13.5 \mu\text{g m}^{-3} \text{Mm sr}$ , which was derived previously from lidar measurements and microphysical inversions in Leipzig. For the flux profiles, a linear behaviour between the surface flux and the entrainment flux (at the boundary-layer top) is expected from theory. While this seems to be the case down to 300 m, below the flux approaches zero. This might be due to the fact that the small eddies responsible for the flux at the surface were not fully resolved by the 10-s lidar profiles. This effect however has to be investigated further.

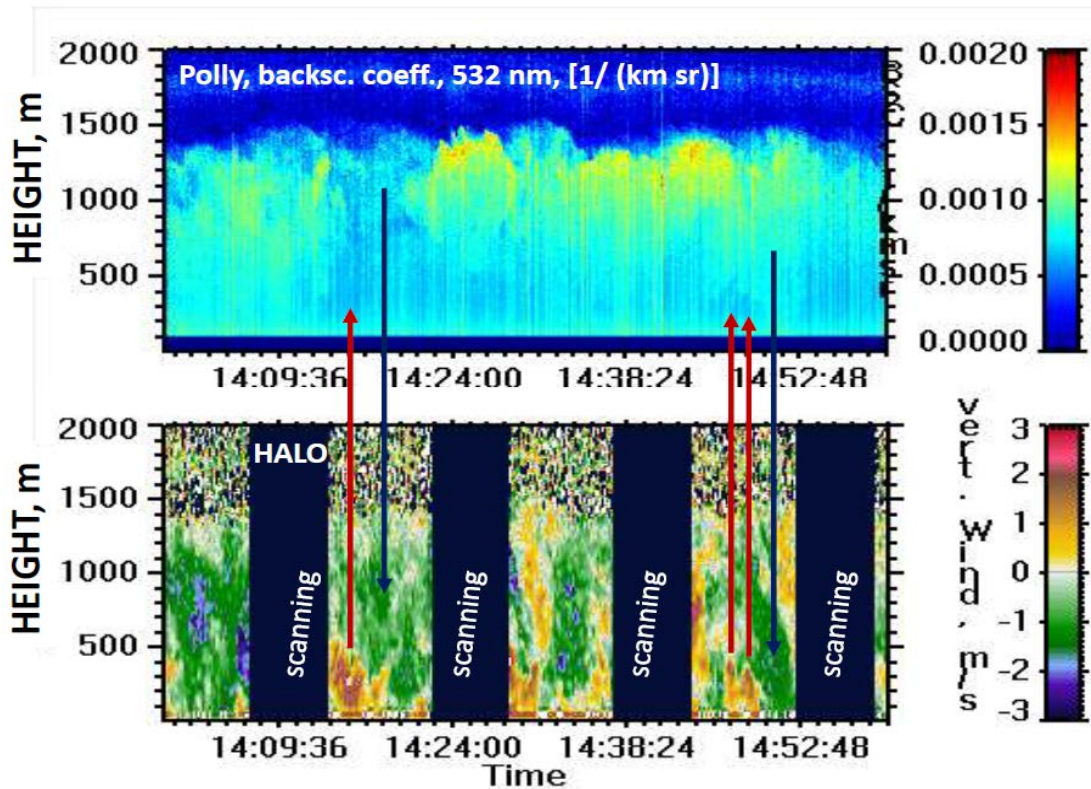


Figure 9. Profiles of the backscatter coefficient (top) and corresponding vertical wind (bottom) between 1400 and 1500 UTC on 23 August.

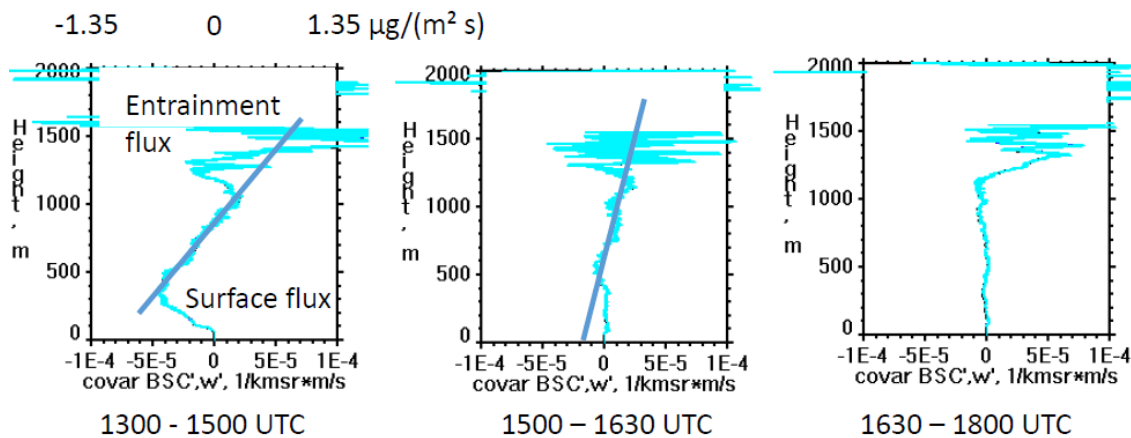


Figure 10. Profiles of the vertical aerosol mass flux from lidar measurements in Košetice on 23 August 2018 for three different periods.

### Hyytiälä (Finland, UHEL)

SMEAR II (*Station for Measuring Ecosystem-Atmosphere Relations*) is located in Hyytiälä in Southern Finland. The station is located in a boreal forest with majority of the tree species being pine trees. In Hyytiälä (Finland), the potential for concurrent Doppler lidar and tower-based fluxes has been available continuously since the deployment of the Doppler lidar in 2013. In addition, during the BAEEC (Biogenic Aerosols—Effects on Clouds and Climate) campaign in spring 2014, measurements with a co-located Halo Streamline Doppler Lidar and PollyXT aerosol lidar were conducted, together with EC measurements using Metek USA-1 and TSI3010 at a height of 23 meters were measured. However, the low Doppler lidar instrument sensitivity and low aerosol loading at the sites, combined with the PollyXT aerosol lidar having significant overlap issues in the shallow boundary layer meant that reliable lidar-based fluxes have been difficult to derive and characterise.

On 26 September 2015, an additional sonic anemometer (Metek USA-1) was installed at the top of the tall mast at 125 m, and the Doppler lidar sensitivity was improved after routine maintenance.

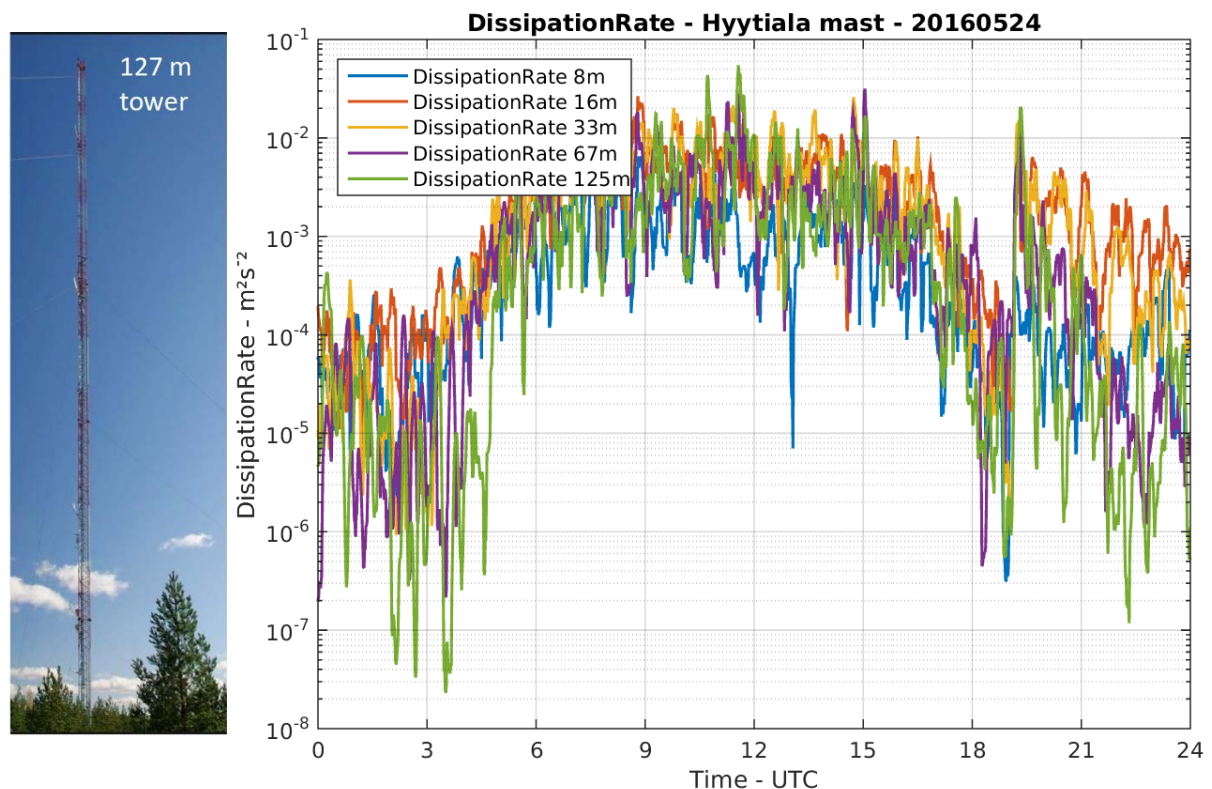


Figure 11. Dissipation rate retrieved from sonic anemometers at 5 levels on the tall mast at Hyytiälä on 24 May 2016.

The first task performed at Hyytiälä was to test the ability to retrieve turbulent parameters from Doppler lidar systems. To do this we evaluated the Doppler lidar dissipation rate retrieval of O'Connor et al. (2010) by comparison with dissipation rates retrieved from sonic anemometer measurements on the tall mast at 5 levels: 8, 16, 33, 67, 125 m. Sonic anemometer dissipation rates were obtained using 'standard' flux processing software from ICOS with 10 minute resolution (Fig. 11). Note that the sonic anemometer at 8 m is within the tree canopy. The uncertainty in dissipation rate is estimated to be about a factor of 5.

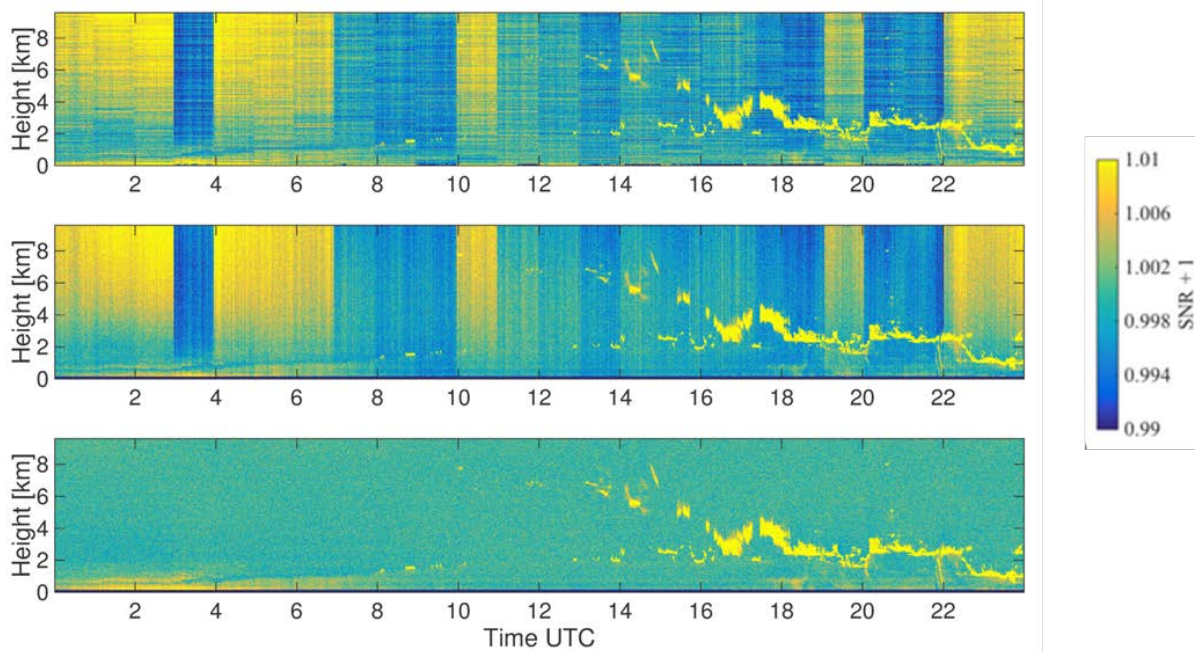


Figure 22. An example of post-processing of the Halo Doppler lidar SNR using the method of Manninen et al. (2016).

The retrieval method of O'Connor et al. (2010) derives dissipation rate from the Doppler velocity variance. In addition to the 'true' turbulent Doppler velocity variance, the observed Doppler velocity variance contains contributions for other sources, which must be accounted for. A major contribution is the uncertainty in the velocity estimate itself, which is a function of the signal-to-noise ratio, SNR. Reliable Doppler velocity uncertainties from the Halo Doppler lidar require post-processing of the SNR (Fig. 12) using the method of Manninen et al. (2016), especially in low SNR conditions. The uncertainties in Doppler lidar dissipation rate estimates are SNR-dependent and expected to range between a factor of 1.5 and 5.

An example of the intercomparison between Doppler lidar and sonic anemometer-retrieved dissipation rates is given in Fig. 13. At the 125 m level, where the measurements coincide, dissipation rate values agree within a factor of 5, and show the same behaviour over time, with the rapid mixed-layer growth starting at 0430 UTC and the mixed-layer decaying around 1800. Turbulent signatures in the evening (after 1900), attributed to a low-level jet, are also seen in both. The sonic anemometer data shows turbulent mixing during the entire period close to the surface. The minimum range of the Doppler lidar is about 90 m, which means that these low-level features are missed by vertically-pointing operation. A proxy for dissipation rate can be obtained using low-elevation scanning (Vakkari et al., 2015) enabling retrievals below 90 m. The same features are found in both the sonic anemometer and the low-elevation scanning, showing that the scanning data can be used to reliably determine very low mixing-level heights, but the dissipation rate uncertainties from scanning Doppler lidar data are a factor of 10 or more and highly dissipation rate and SNR-dependent. Such intercomparisons provide confidence in the ability of Doppler lidar to reliably capture turbulent parameters within the boundary layer.

During this period the Doppler lidar at Hyytiälä was operated with 10 second integration time, producing a temporal resolution of 20 s, due to interleaving between co and cross polarisations. Horizontal winds were obtained every 15 minutes using either a VAD scan at 30 degrees elevation from horizontal, or a Doppler Beam Swing (DBS) scan at 70 degrees elevation from horizontal.

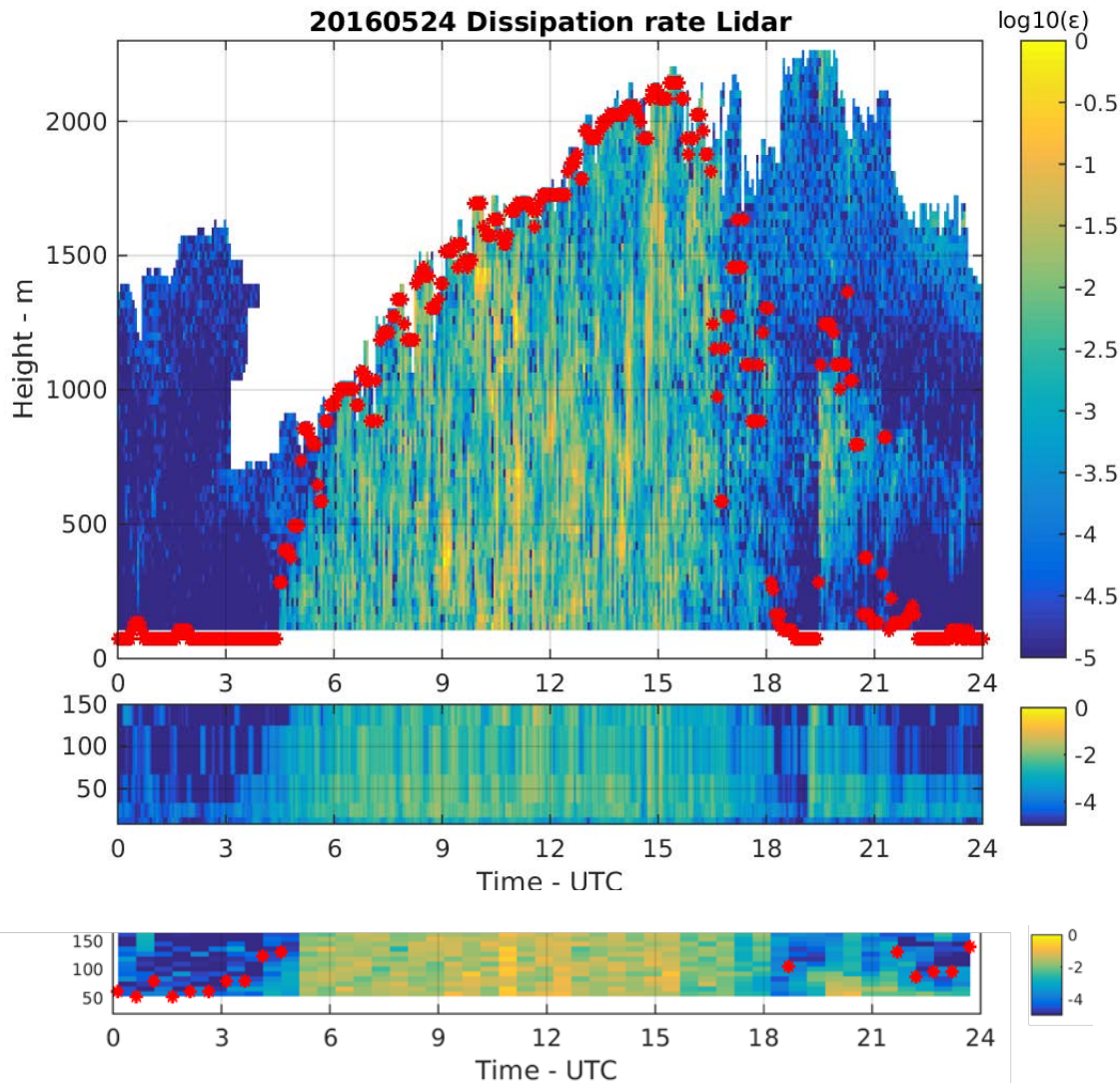


Figure 33. Dissipation rate retrieved from vertically-pointing Doppler lidar (top panel), sonic anemometers (centre panel) and low-elevation Doppler lidar scanning (lower panel) at Hyytiälä on 24 May 2016. The same colour scale is used for all dissipation rate retrievals. Red dots indicate the mixing-level height derived from the Doppler lidar turbulent parameters.

In the absence of an aerosol lidar during this period, the covariance method of  $(\beta'w')$  was applied to the Doppler lidar only. Results from 2 consecutive clear-sky days are displayed in Figs. 14-17. Both days show similar patterns in the vertical profile of  $(\beta'w')$ , a proxy for the aerosol mass flux  $F(z)$ : the early morning profile (0600-0800 in Figs. 15 and 17) displays a positive region between the surface and about 300 m, which transforms during the day to a profile similar to that found at Košetice (Fig. 10) in the afternoon. The inference is that, during the afternoon, the surface and the free-troposphere are sinks, but the surface is acting as a source during the morning. However, as previously explained, the flux always approaches zero close to the surface which may be a consequence of transport via the smallest eddies not being adequately captured by the Doppler lidar due to the volume measurement and 10-s sampling times.

The maximum magnitude of the covariance term is at least a factor of 10 lower than for Košetice and Granada, suggesting aerosol fluxes that are also an order of magnitude smaller (given a similar covariance->mass flux conversion factor). This is not surprising as the aerosol mass loading itself is also an order of magnitude lower. Note that attenuated backscatter was used in the calculation of covariance rather than backscatter coefficient due to the uncertainty in the lidar ratio necessary for calculating extinction at this

particular lidar wavelength. However, the total aerosol extinction was low on these two days, with the sunphotometer suggesting an AOD of about 0.06 at a wavelength of 1620 nm.

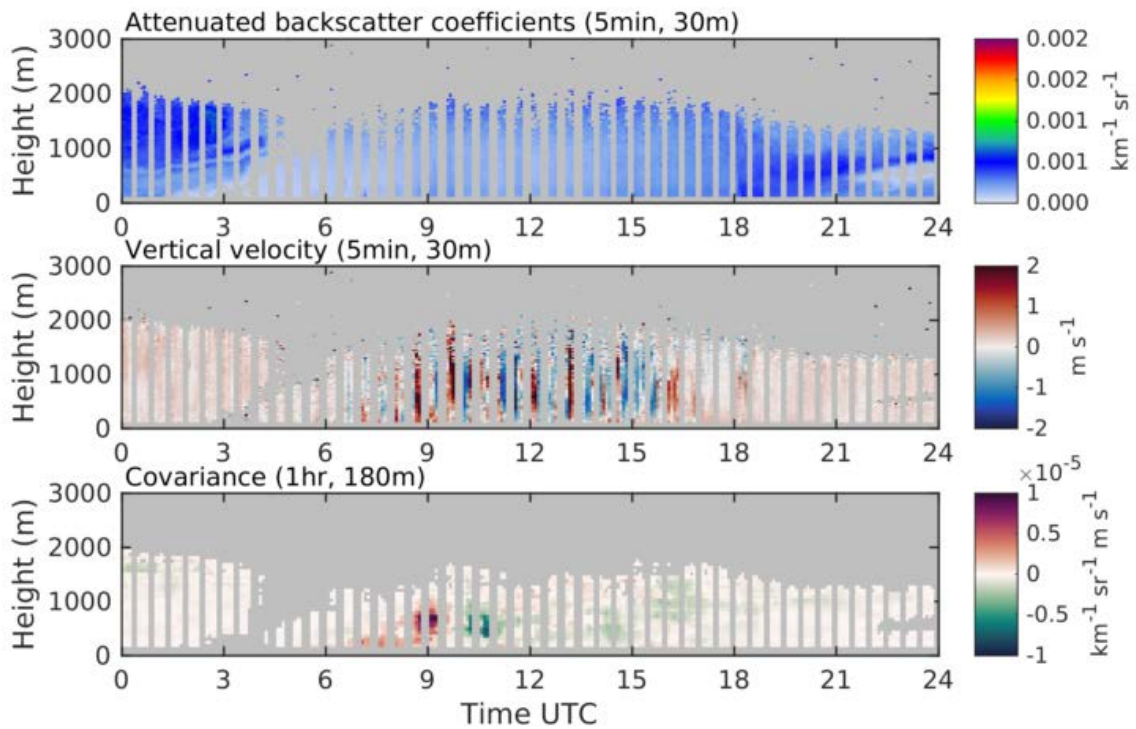


Figure 44. Time-height profiles of attenuated backscatter coefficient, vertical Doppler velocity and  $\beta'w'$  covariance retrieved from vertically-pointing Doppler lidar at Hyttiälä on 6 May 2016.

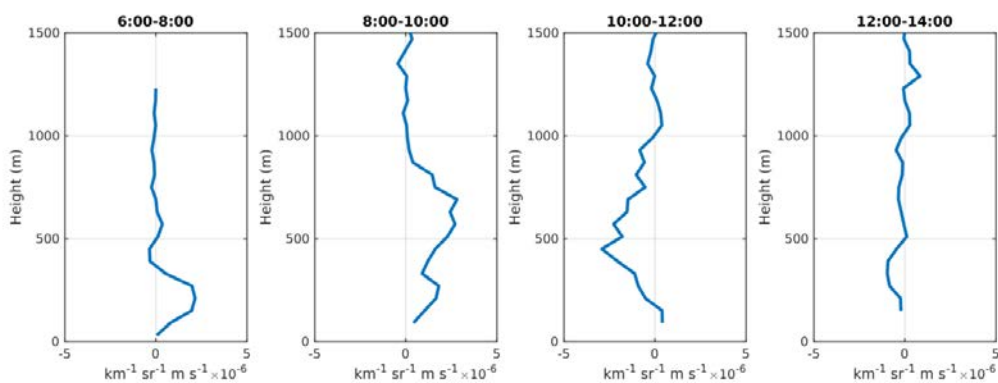


Figure 55. Vertical profiles of  $\beta'w'$  covariance averaged over 2 hours from vertically-pointing Doppler lidar at Hyttiälä on 6 May 2016.

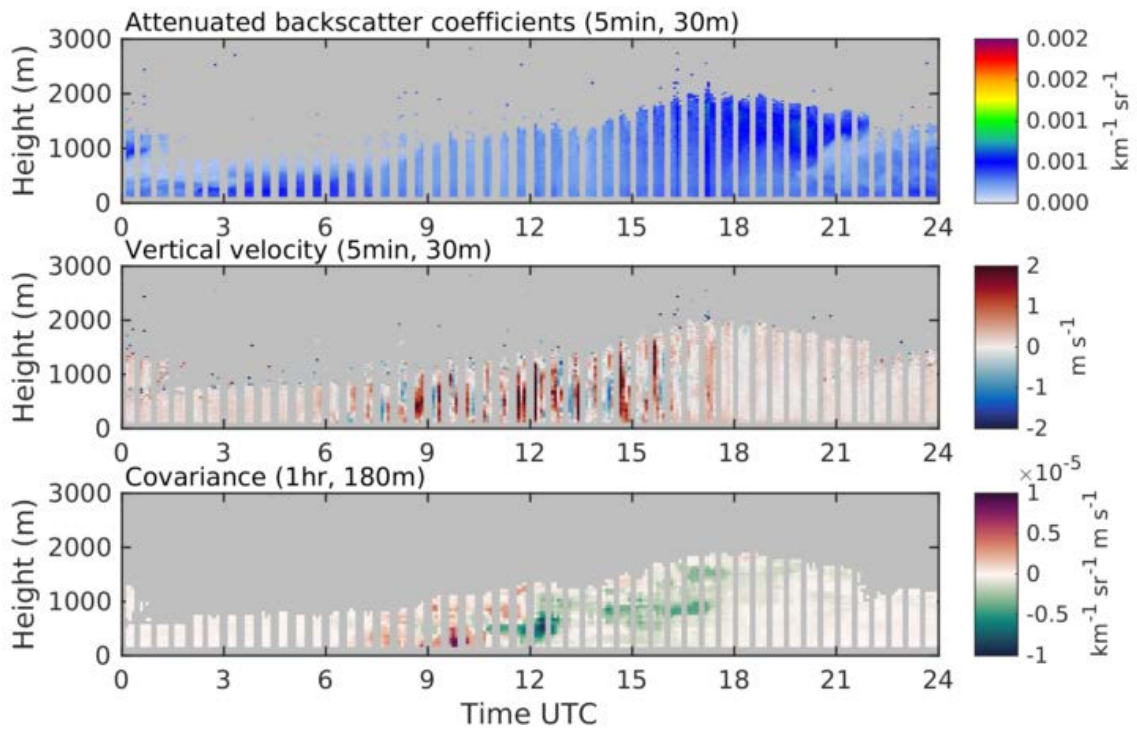


Figure 66. Time-height plots of attenuated backscatter coefficient, vertical Doppler velocity and  $\beta'w'$  covariance retrieved from vertically-pointing Doppler lidar at Hyttiälä on 7 May 2016.

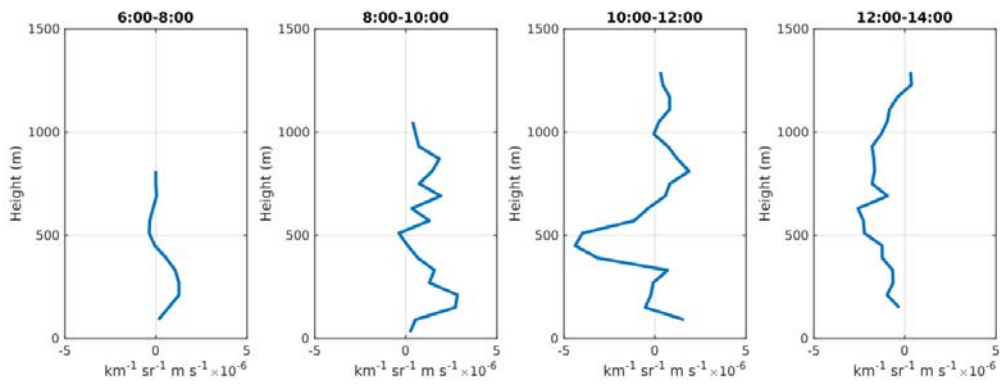


Figure 77. Vertical profiles of  $\beta'w'$  covariance averaged over 2 hours from vertically-pointing Doppler lidar at Hyttiälä on 7 May 2016.

### Pallas (Finland, FMI)

Pallas research station (67.973°N, 24.116°E) is located 170 km north of the Arctic Circle, partly in the area of Pallas-Yllästunturi National Park and at the northern fringe of the boreal vegetation zone. Pallas is a northern node of the Pallas-Sodankylä research infrastructure of the Finnish Meteorological Institute, the other node being located in the Sodankylä Arctic Research Centre. The main atmospheric measurements are conducted on top of a barren fell called Sammaltunturi (565 m above mean sea level). A supporting ecosystem site, Kenttäröva, is situated in a pine forest on a hill (347 m above mean sea level) that is circa 60 m above the surrounding plain and within 6 km of the Sammaltunturi fell.

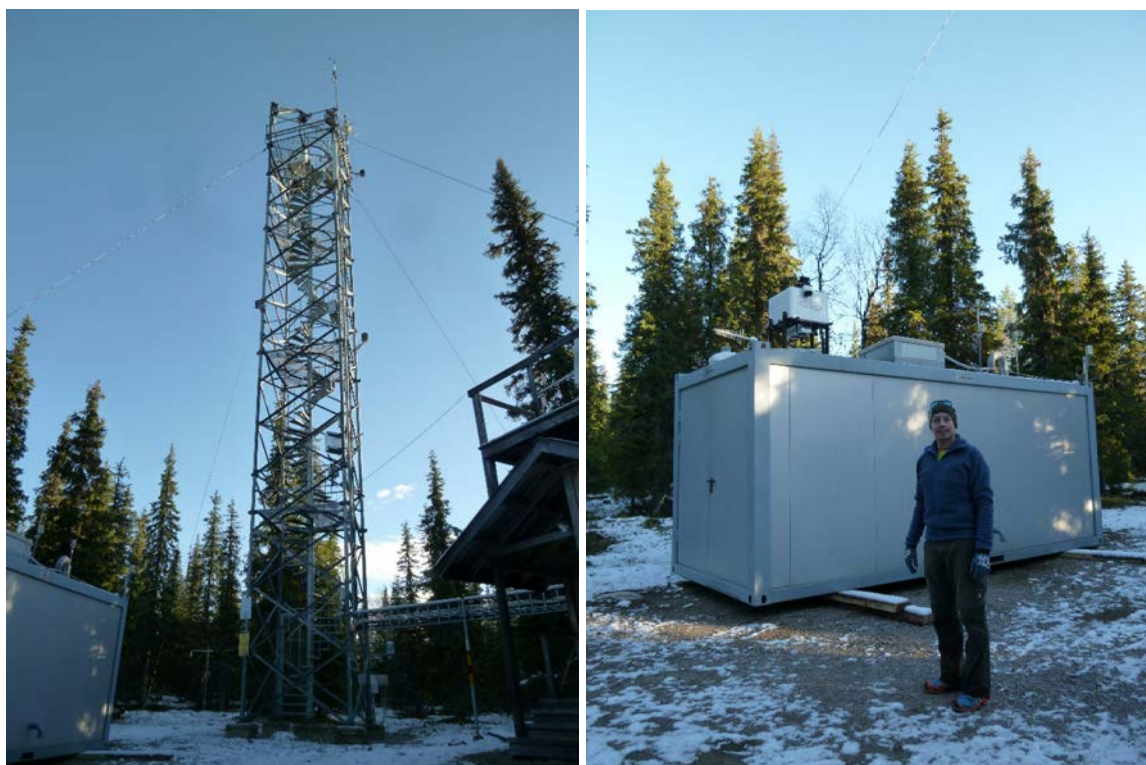


Figure 88. Instruments deployed at Kenttäröva, in northern Finland for the PACE2015 campaign. The tower (left) extends above the tree canopy, PollyXT and Halo Streamline Doppler lidar were operated within 2 m of each other.

At Pallas (Finland), simultaneous particle flux measurements using both *in-situ* and remote sensing techniques were conducted at the Kenttäröva station during late autumn of 2015 as part of the PACE (*Pallas Cloud Experiment*) campaign. The *in-situ* measurement setup consists of an ultrasonic anemometer (Metek USA-1) and a CPC (TSI3776). Low total particle number concentrations and problems with data stream synchronization has proven to be challenging with the present setup. For boundary layer fluxes, a Halo Streamline Doppler Lidar and PollyXT multi-wavelength Raman aerosol lidar were operated during the PACE 2015 campaign (Fig. 18).

Similar to the low counts obtained from the CPC at this Arctic site, the clean air also means that the lidar signals are very weak. Since the measurement uncertainty for both Doppler velocity and attenuated backscatter is directly related to the signal-to-noise ratio (SNR), this results in large measurement uncertainties. Usually, this issue would be solved by using long integration times, but this would not be appropriate for measuring fluxes. This is evident in the dissipation rate uncertainties calculated for 2 consecutive days in Pallas shown in Figs. 19 and 20. The first example (Fig. 19) shows promise, with enough signal to at least calculate dissipation rate. However, the second example (Fig. 20) was more representative of the campaign and shows the difficulty of measuring any aerosol in a clean environment.

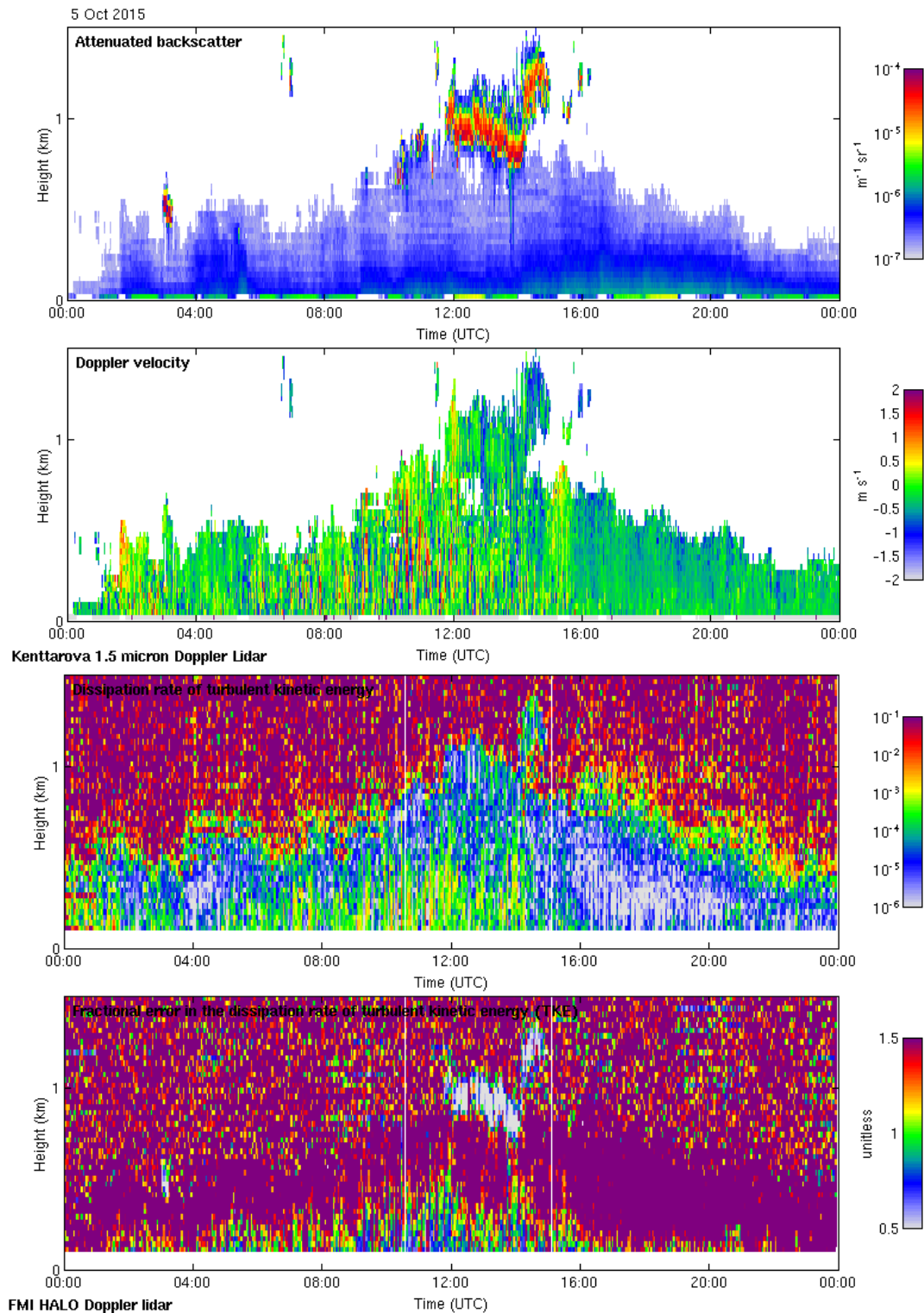


Figure 99. Time-height plots of attenuated backscatter coefficient, vertical Doppler velocity, dissipation rate, and uncertainty in dissipation rate retrieved from vertically-pointing Doppler lidar at Kenttäröva on 5 October 2015. Uncertainty estimate for dissipation rate is expressed in percentage terms, i.e. 0.5 is equivalent to 50 %, 1 is 100% and 1.5 is 150 %, hence only reliable data is in-cloud or in the shallow well-mixed boundary layer during the day.

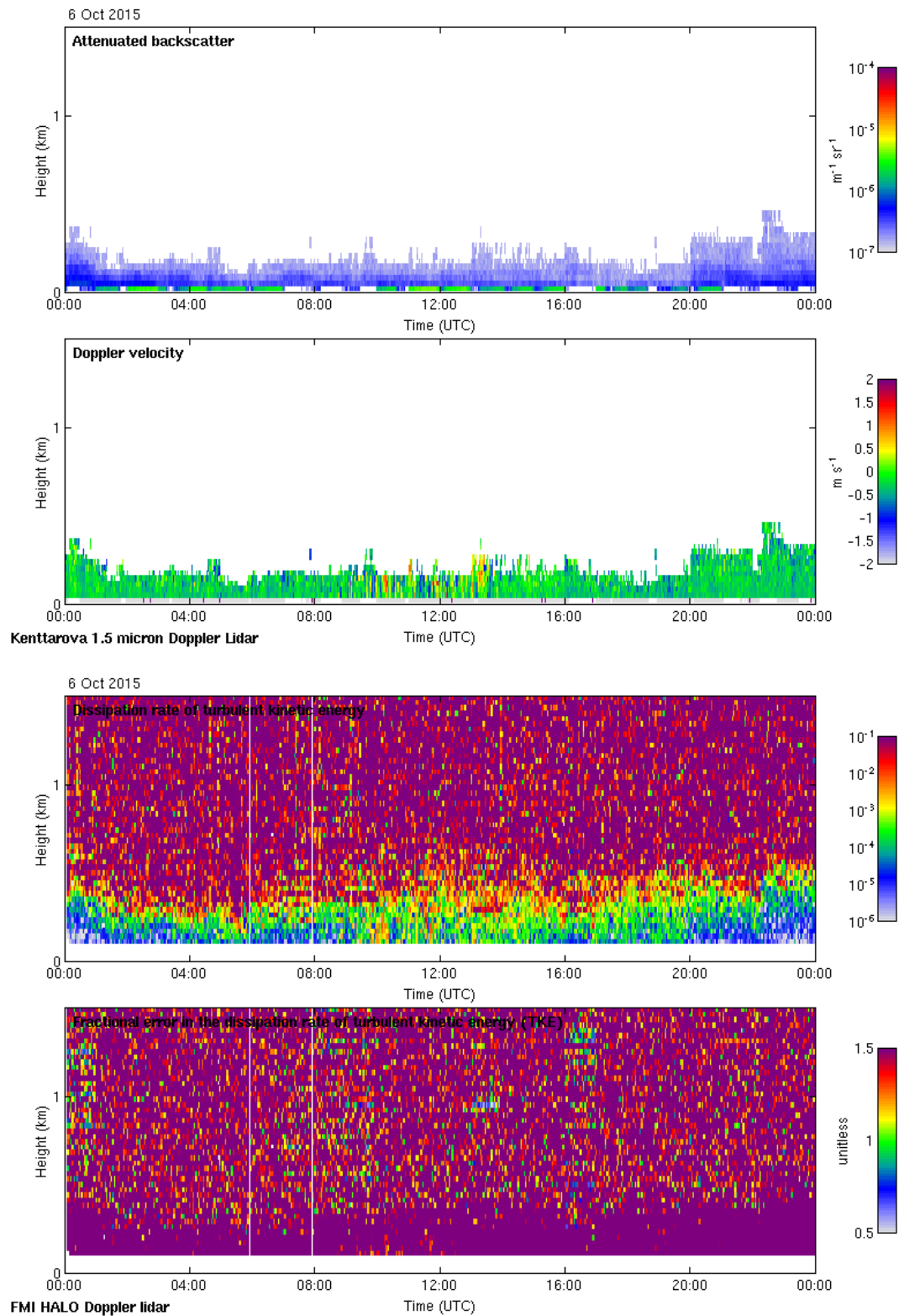


Figure 20. Time-height plots of attenuated backscatter coefficient, vertical Doppler velocity, dissipation rate, and uncertainty in dissipation rate retrieved from vertically-pointing Doppler lidar at Kenttäröva on 6 October 2015. Uncertainty estimate for dissipation rate is expressed in percentage terms, i.e. 0.5 is equivalent to 50 %, 1 is 100% and 1.5 is 150 %, hence no reliable data for this day.

The boundary layer was also very shallow during much of the measurement campaign, as was expected for this Arctic site. A shallow boundary layer poses additional complications for simultaneous measurements by a Doppler lidar and an aerosol lidar, related to the minimum range that each instrument can obtain reliable data from. For Doppler lidars, this is typically 90 m and can be mitigated by scanning, whereas overlap issues for more powerful aerosol lidars may limit the minimum range to 300 m or more. There is usually no useful Doppler lidar signal outside the boundary layer, so the challenge is to make aerosol lidar measurements within a shallow boundary layer that may be less than 300 m deep.

Recently, FMI has purchased a new Doppler lidar with significant sensitivity enhancements, which is planned to be deployed in Pallas for a new measurement campaign. Initial results from a deployment elsewhere in Finland look promising.

## Conclusions

The aim of Task 12.4 was to conduct measurement campaigns to determine whether profiles of aerosol particle fluxes could be obtained in the planetary boundary layer using active remote sensing in the form of lidar. Co-located Doppler and aerosol lidars were operated simultaneously during measurement campaigns that have been performed at six locations in different parts of Europe.

Numerous lessons were learnt from these campaigns, including optimum measurement setups, scanning and temporal resolution strategies, together with dealing with challenges such as instrument sensitivity, instrument minimum range, and ensuring accurate timestamping.

Preliminary estimates for the vertical profile of particle fluxes have been demonstrated at four sites: Agora, Granada, Hyytiälä and Košetice. The methodology on how to derive the particle fluxes is still under development, but the preliminary measurements look promising and suggests that reasonable particle flux profiles can be obtained in the planetary boundary layer. A full assessment of the methodology and appropriate uncertainty estimates is still required, including accounting for Doppler lidar telescope focus function or aerosol lidar overlap function, particle size changes due to humidity changes, extinction properties at the Doppler lidar wavelength, autocorrelation of two timeseries (whether correcting for timestamping or for instrument separation). An additional issue to explore is to determine the contribution to the total particle flux from small eddies that may be missed due to instrument volume and temporal characteristics.

The campaign in Pallas in Finnish Lapland was shown to be too clean for the current instrumentation to be able to detect mass fluxes at the site. New post-processing of the Doppler lidar data shows that it is possible to retrieve dissipation rates but with very large uncertainties. A similar issue was found at Hyytiälä for the initial campaign, but improved sensitivities and new post-processing of the Doppler lidar shows much more potential, even with low aerosol loading. The CINDI-2 measurement campaign at Cabauw had some challenges due to an issue with the wind profiler that was used and the analysis of this dataset is still ongoing.

## References

- Engelmann R., Wandinger U., Ansmann A., Müller D., Zeromskis E., Althausen D. and Wehner B. (2007). Lidar observations of the vertical aerosol flux in the planetary boundary layer. *J. Atmos. Ocean Technol.* **25**, 1296-1307.
- Kinne S., Schulz M., Textor C., Guibert S., Balkanski Y., Bauer S.E., Berntsen T., Berglen T.F., Boucher O., Chin M., Collins W., Dentener F., Diehl T., Easter R., Feichter J., Fillmore D., Ghan S., Ginoux P., Gong S., Grini A., Hendricks J., Herzog M., Horowitz L., Isaksen I., Iversen T., Kirkevåg A., Kloster S., Koch D., Kristjansson J.E., Krol M., Lauer A., Lamarque J.F., Lesins G., Liu X., Lohmann U., Montanaro V., Myhre G., Penner J., Pitari G., Reddy S., Seland O., Stier P., Takemura T. and Tie X. (2006). An AeroCom initial assessment – optical properties in aerosol component modules of global models. *Atmos. Chem. Phys.* **6**, 1815-1834.
- Klett J.D. (1981). Stable analytical inversion solution for processing lidar returns. *Appl. Opt.*, **20**, 211–220.
- Manninen, A. J., O'Connor, E. J., Vakkari, V., and Petäjä, T. (2016): A generalised background correction algorithm for a Halo Doppler lidar and its application to data from Finland, *Atmos. Meas. Tech.*, **9**, 817-827, <https://doi.org/10.5194/amt-9-817-2016>.
- Moreira G. de A., Guerrero-Rascado J.L., Benavent-Oltra J.A., Ortiz-Amezcuca P., Román R., Esteban Bedoya-Velásquez A., Bravo-Aranda J.A., Olmo-Reyes F.J., Landulfo E. and Alados-Arboledas L. (2018). Analyzing the turbulence in the Planetary Boundary Layer by the synergic use of remote sensing systems: Doppler wind lidar and aerosol elastic lidar. *Atmos. Chem. Phys. Discuss.*, doi: 10.5194/acp-2018-276.
- O'Connor, E.J., A.J. Illingworth, I.M. Brooks, C.D. Westbrook, R.J. Hogan, F. Davies, and B.J. Brooks (2010): A method for estimating the turbulent kinetic energy dissipation rate from a vertically pointing Doppler lidar, and independent evaluation from balloon-borne in situ measurements. *J. Atmos. Oceanic Technol.*, **27**, 1652–1664, <https://doi.org/10.1175/2010JTECHA1455.1>
- Vakkari, V., O'Connor, E. J., Nisantzi, A., Mamouri, R. E., and Hadjimitsis, D. G. (2015): Low-level mixing height detection in coastal locations with a scanning Doppler lidar, *Atmos. Meas. Tech.*, **8**, 1875-1885, <https://doi.org/10.5194/amt-8-1875-2015>.